

# INVESTIGATION OF THE LARGE SCALE STRUCTURES IN THE TURBULENT MIXING LAYER DOWNSTREAM A THICK PLATE

Laurent Perret, Joël Delville and Jean-Paul Bonnet  
Laboratoire d'Etudes Aérodynamiques - UMR CNRS 6609  
Université de Poitiers - ENSMA  
C.E.A.T., 43, route de l'Aérodrome F-86036 Poitiers - France

## ABSTRACT

Experiments were performed in an incompressible plane mixing layer past a blunt trailing edge for a Reynolds number based on the splitter plate thickness of  $\mathcal{O}(10^4)$ . The influence of the trailing edge geometry on the mixing layer development was investigated with two-point hot wire measurements which permit us to perform a Proper Orthogonal Decomposition (POD) of the flow. The blunt trailing edge wake was found to be responsible for a strong modification of the organization of the flow. Compared to a conventional mixing layer, the self-similar region was shifted downstream, the scale of the large structure are governed by the trailing edge thickness and all the statistical quantities such as the Reynolds stress profiles or the POD modes exhibit a stream-wise evolution dominated by the wake characteristics over the mixing layer behaviour in the near region.

## INTRODUCTION

Several authors have shown that the development of the mixing layer resulting of the interaction of two different velocity streams at the trailing edge of a splitter plate is very sensitive to the inflow conditions. Parameters such as the momentum thickness of the boundary layers at the trailing edge or their laminar or turbulent state have a strong influence on the downstream behaviour of the flow, especially on the growth rate of the mixing layer and on the location of the self-similar region. In particular, Dziomba and Fiedler (1985) showed experimentally the importance of the trailing edge thickness  $h$ . In fact, they found that if this parameter exceeds 50% of the sum of the boundary layer displacement thickness  $\delta_1$  on the splitter plate, its influence becomes significant and modifies both the spreading rate and the characteristic frequencies of the flow, the instability frequency of the wake becoming dominant. They also confirmed the theoretical demonstration by Michalke and Shade (1963) of the strong influence of the wake component of the longitudinal velocity profiles on the Strouhal number. Boldman *et al.* (1976) made both an experimental and a numerical investigation of the influence of the external velocity ratio  $r = U_a/U_b$  ( $U_a > U_b$ ) on the development of the mixing layer behind a blunt trailing edge. They showed that the spatial organization of the flow as well as the vortex shedding frequency depend on velocity ratio. As this parameter decreases to zero the periodic vortex shedding indicative of a wake flow tends to disappear. They measured a Strouhal number about 0.2 based on the trailing edge thickness and the average of the external velocities. In his study of the plane mixing layer development, Metha (1991) found that the splitter plate wake and its complex interaction with the mixing layer plays a dominant role, especially in the way the self-similar state is reached. Koch (1985) investigated

self-excited wake flow development (more particularly flows past a blunt edged flat plate) by means of stability analysis. He showed that the nature of the flow instability which can be either convective or absolute is directly related to the asymmetry of the initial conditions, namely the external velocity ratio and the difference of the characteristics of the boundary layers on the dividing plate.

Quantities such as the spreading rate or the characteristic frequency depend on the inflow conditions but are also characteristic of the large scale structures of the flow. As a consequence, techniques such as conditionnal and structural averaging (Antonia, 1981) or Proper Orthogonal Decomposition (POD) introduced by Lumley (1967) can be used to study the influence of the trailing edge geometry on the downstream development of the flow.

In the present work, we have analysed the influence of the wake effect of the splitter plate trailing edge on the downstream evolution of a fully developed turbulent mixing layer. In this case the of a high ratio between the trailing edge thickness and the displacement thickness of the boundary-layers  $h/\delta_1$  is about 10. This kind of flow is of interest because it is expected to exhibit different behaviours, presenting simultaneously two types of global instability. Indeed, an absolute instability due to the splitter plate wake influence and a convective instability characteristic of the mixing layer behaviour can be found simultaneously in such a flow (Koch, 1985).

## EXPERIMENTAL SET UP

The experiments were carried out in an open wind-tunnel at CEAT/LEA in Poitiers, France. The two-dimensional subsonic turbulent mixing layer had a high speed velocity  $U_a$  of 35.2 m/s and a low speed velocity  $U_b$  equal to 23.8 m/s (velocity ratio  $r = 0.67$ ). The height of the trailing edge  $h$  was equal to 19 mm. The Reynolds number based on the difference of velocity between the two flows and  $h$  is  $Re = h\Delta U/\nu \simeq 14,400$ . A sketch of the mixing layer together with the coordinate system used in this study is shown in figure 1. In order to be able to quantify the wake effect, the splitter plate trailing edge can be either blunt (configuration named here thick mixing-layer (TML)) or beveled (or conventional mixing layer (CML)). The half-angle of the bevel ( $12^\circ$ ) was chosen to avoid flow detachment in this region. The experiments were systematically performed in both configurations.

The measurements were performed at different downstream locations (from  $x/h = 5.25$  to  $x/h = 42.1$ ) by using hot wire anemometry. A rake of 19 non-uniformly spaced "X" wires probes was used to obtain both the longitudinal and the transversal (normal to the plate) velocity components. The probes were placed symmetrically about the

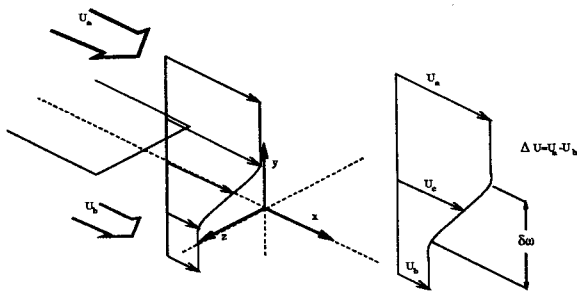


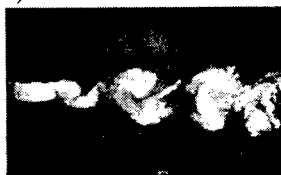
Figure 1: Plane mixing layer coordinates.

mixing layer axis with a separation of 4.0 mm near the center of the shear layer and 8.0 mm in the external region, the rake spanning approximately 93 mm (4.9  $h$ ). The diameter of the wires was 2.5  $\mu\text{m}$  and the sensing length was about 0.5 mm. The 38 velocity signals were simultaneously sampled at 50 kHz after low pass filtering at 25 kHz.

### FLOW VISUALISATIONS

Flow visualisations were performed by injecting smoke into the flow at the trailing edge of the splitter plate. From instantaneous photographs (Fig 2), the thick mixing layer clearly exhibits a strong organization and larger scales when compared to the conventional mixing layer. More particularly, two rows of opposite signed vortices located at the top and the bottom edges of the trailing edge of the splitter plate can be observed in figure 2a). The top and bottom vortices are not strictly alternating like in a wake but seem to be almost vertically aligned with the low speed structures being consumed by high speed ones. Hence they tend to merge downstream to form only one row. It results in an large increase of the growth rate of the shear layer.

a) TML



b) CML

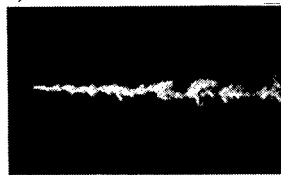


Figure 2: Instantaneous flow visualisations (at the same scale) (nearly 13.7  $x/h \times 8.4 x/h$ ).

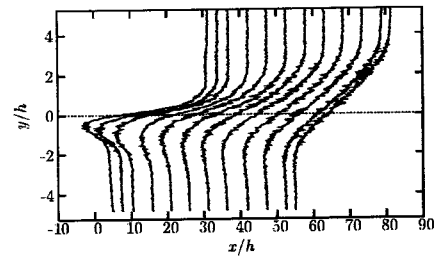
### STATISTICAL RESULTS

#### Mean Velocity Profiles

The mean longitudinal velocity profiles (Fig 3) measured at different streamwise locations show the strong influence of the wake effect when a blunt trailing edge is used. A velocity defect can be observed until  $x/h \simeq 52$ . As a consequence, the self-similarity region is reached very far downstream. Moreover, it is noticeable that the thick mixing layer develops essentially on the high velocity side of the flow. In both their experimental and numerical studies of the vortex shedding from a blunt trailing edge with unequal external mean velocities, Boldman *et al.* found (1976) also such a behaviour when the mean velocity ratio is below 1. To quantify the growth rate of the mixing layer, the vorticity thickness defined as:

$$\delta_\omega = \Delta U / (du/dy)_{max} \quad (1)$$

a) TML



b) CML

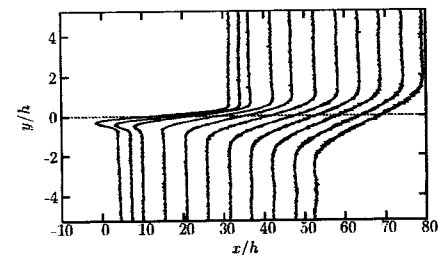


Figure 3: Mean longitudinal velocity profiles

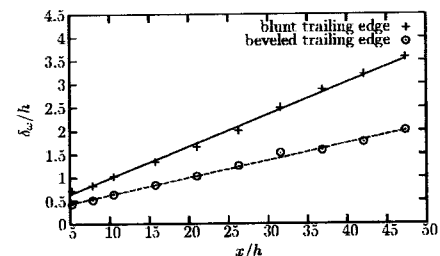


Figure 4: Longitudinal evolution of the vorticity thickness  $\delta_\omega$ . +: blunt trailing edge, o: beveled trailing edge.

can be computed. The streamwise evolution of  $\delta_\omega$  is plotted in figure 4, confirming the strong expansion of the thick mixing layer at about twice the rate of the conventional mixing layer (respectively  $d\delta_\omega/dx = 0.0684$  and  $0.0371$ ).

#### Longitudinal Evolution of the Reynolds stress

The Reynolds shear stress profiles obtained when a blunt trailing edge is used are plotted as a function of the streamwise distance in figure 5. As with the mean velocity profiles, they exhibit two different behaviours revealing the different regions involved in this flow:

- In the near wake ( $x/h < 16$ ), two peaks of opposite sign can be seen. The high-speed side has a negative peak whereas the other side has a positive extremum decreasing with the longitudinal distance and eventually disappears. It is remarkable that the positive peak was more important in magnitude than the negative in the near region and tends rapidly to zero.
- For  $x/h$  greater than typically 16, the effect of the wake disappears and is overcome by the mixing layer influence. The Reynolds stress profiles have the classical shape found for a conventional mixing layer with only one negative extremum.

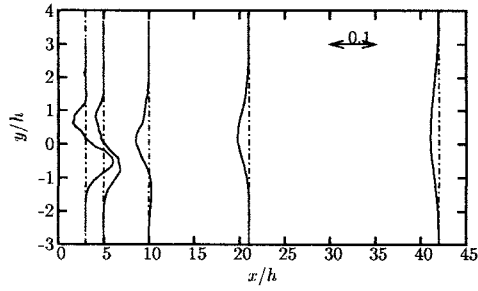


Figure 5: Streamwise evolution of the Reynolds stress  $\overline{u'v'}/\Delta U^2$  in the TML case.

Metha (1991) found the same type of behaviour in his study of the effect of velocity ratio on plane mixing layer development, showing that the magnitude of the low-speed side Reynolds stress peak is an increasing function of the velocity ratio. For all the velocity ratio Metha (1991) explored, the high-speed side extremum was found to be always greater than the second peak which is contrary to our results. This difference can be attributed to the fact that he used a thinner trailing edge relative to  $\delta_1$  reducing the strength of the wake effect.

#### Longitudinal Evolution of the Turbulent Intensity

Figure 6 shows the longitudinal evolution of the maxima of  $u'$  and  $v'$  intensities (respectively  $\sqrt{u'^2}|_{max}$  and  $\sqrt{v'^2}|_{max}$ ) for the two flow configurations. It's noticeable that the maximum levels of the fluctuation of  $u$  and  $v$  are always larger in the case of the blunt trailing edge. These quantities seem to converge to the same value downstream. Moreover, contrary to the conventional case,  $\sqrt{v'^2}|_{max}$  is larger than  $\sqrt{u'^2}|_{max}$  until  $x/h = 21$  for the thick mixing layer. The wake effect produces a strong excitation of the flow which leads to a higher turbulent intensity and shifts downstream the self-similarity region where  $\sqrt{u'^2}|_{max}$  and  $\sqrt{v'^2}|_{max}$  are supposed to be constant with respect to the longitudinal location. These results can be compared to those of Metha (1991). In the case of the conventional mixing layer the evolution of the streamwise and transversal velocity fluctuation maxima are quite similar both in qualitative and quantitative manners. As far as the thick mixing layer is concerned, the evolution of the maximum of  $\sqrt{u'^2}$  is surprisingly closer to the measurements of Metha (1991) when  $r = 0.9$ . However, it is not the case for the transversal component for which the level of the maximum is higher in the present study.

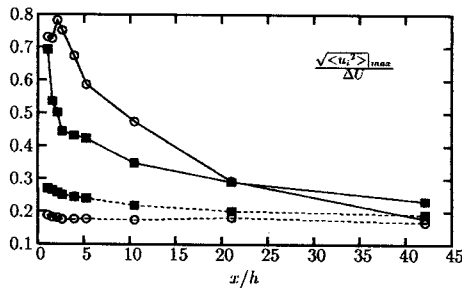


Figure 6: Longitudinal evolution of the maxima of fluctuation of the longitudinal velocity (■) and the transversal velocity (○).— TML, - - - CML.

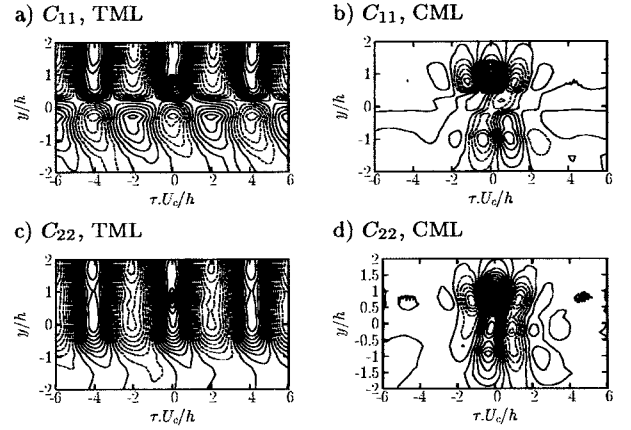


Figure 7: Spatio-temporal correlation coefficients of the longitudinal (a) and b)) and the transversal (c) and d)) velocity components ( $x/h = 5.25$ ), — positive correlations, - - - negative correlations. a) and c) TML, b) and d) CML

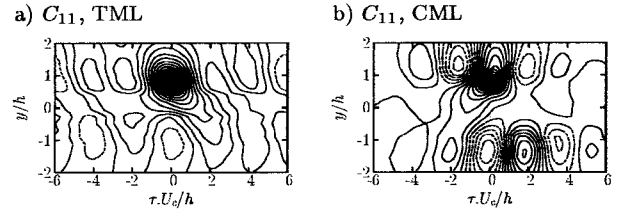


Figure 8: Spatio-temporal correlation coefficients of the longitudinal velocity component ( $x/h = 21$ ), — positive correlations, - - - negative correlations. a) TML, b) CML

#### Space-Time Correlations

Space-time correlation coefficients were obtained with the rake of X hot wires and were computed for each velocity component as follow:

$$C_{ii}(y, y', \tau) = \frac{\langle u_i(y, t)u_i(y', t+\tau) \rangle}{\sqrt{\langle u_i(y, t)^2 \rangle} \sqrt{\langle u_i(y', t)^2 \rangle}}$$

where  $\langle . \rangle$  is the conventional time average. These statistics permit us to characterize the spatio-temporal organization of the flow. Figure 7 shows a typical example of these correlations at  $x/h = 5.25$  for the two flow configurations and both the longitudinal and the transversal velocity components. The reference probe was located at  $y/h = 0.84$ . The  $u$ -component correlations show alternating positive and negative correlated areas both in the temporal and the transverse directions. The thick mixing layer appears to be strongly correlated in time whereas the correlation levels decrease rapidly in the conventional case. The  $v$ -component has the same temporal behaviour but its sign does not change with respect to the  $y$ -direction. It should be pointed that near the plate the level of correlation does not seem to vanish with large temporal separations.

The experiments performed at other downstream locations (see Fig 8 for the correlations of the  $u$ -component at  $x/h=21$ ) show the same type of time-correlation and a similar downstream organization. In the case of the blunt trailing edge, the temporal wavelength of the alternate areas appears to be constant with the streamwise direction with a typical time scale  $\tau_0 U_c/h = 4$ . Indeed, although the correlation levels being less important than upstream,  $\tau_0$  remains constant for both  $x$  values. On the contrary, for the conventional mixing layer, it evolves linearly: the further downstream, the greater the wavelength is. These results confirm that the mixing layer past the blunt trailing edge

is dominated by the wake effect for a long time and the large scales of the flow seem to be governed by the trailing edge thickness. The wake effect is to force the flow in time, the large structures being locked on a specific scale. In the case of the beveled trailing edge mixing layer, the large scale organization is scaled to the local vorticity thickness, then evolves linearly with the downstream location.

## APPLICATION OF POD

### Recalls on the POD

In this section, the Proper Orthogonal Decomposition is briefly presented. More details can be found in Berkooz *et al.* (1993) and Delville (1995). Lumley (1967) first proposed the POD technique to identify the coherent structures in turbulent flows. It consists of extracting from the flow the structure  $\phi(X, t)$  with largest mean-square projection onto the velocity field  $\mathcal{U}(X, t)$ . This maximization problem leads to solve the integral problem of eigenvalues:

$$\int_{\mathcal{D}} R_{ij}(X, X') \phi_j(X') dX' = \lambda \phi_i(X) \quad (2)$$

where  $R_{ij}$  is the space-time correlations tensor over the domain  $\mathcal{D}$ :

$$R_{ij}(X, X') = \langle \mathcal{U}_i(X) \mathcal{U}_j(X') \rangle \quad (3)$$

The fluctuating field can be projected onto the POD basis composed of the  $n$  eigenfunctions  $\phi_i^{(n)}(X)$ :

$$\mathcal{U}_i(X) = \sum_{n=1}^{\infty} a^{(n)} \phi_i^{(n)}(X) \quad (4)$$

Two kind of eigenvalues problems can be solved, depending on the kernel which is used. A *spatial POD* can be performed if the POD kernel is the two-point spatial correlation tensor  $R_{ij}(X, X') = \langle \mathcal{U}_i(X) \mathcal{U}_j(X') \rangle$ . If the kernel is the cross-spectrum spatial correlation tensor  $\Psi_{ij}(X, X', f) = \langle \bar{\mathcal{U}}_i(X, f) \bar{\mathcal{U}}_j^*(X', f) \rangle$  where  $\bar{g}$  is the Fourier transform of  $g$  and  $\bar{g}^*$  is the complex conjugate of  $\bar{g}$ , a *spectral POD* is computed. Note that in the present study, only the transversal direction  $y$  is considered for the decomposition.

### Spatial POD results

In this section, a scalar POD approach is used: each velocity component is computed independantly using the two-point spatial correlation tensor  $R_{ii}(X, X') = \langle \mathcal{U}_i(X) \mathcal{U}_i(X') \rangle$  ( $i$  equal 1 or 2).

Figure 9 shows the first two POD modes of the longitudinal velocity component obtained at different downstream locations for the two mixing layer configurations.

In the case of the beveled trailing edge, the classic behaviour of the first two modes is retrieved (see Delville 1995): the shape of the first mode is approximately a gaussian centered on the mixing layer axis, and the second mode is antisymmetric.

As regards to the thick mixing layer, the shape of the first two modes depends on the longitudinal position considered:

- when the longitudinal distance from the trailing edge is greater than typically  $16h$ , the shapes of the first two modes are similar to the conventionnal case.
- For  $x/h$  between 0 and 15.8, the first mode is almost antisymmetric whereas the second one looks more

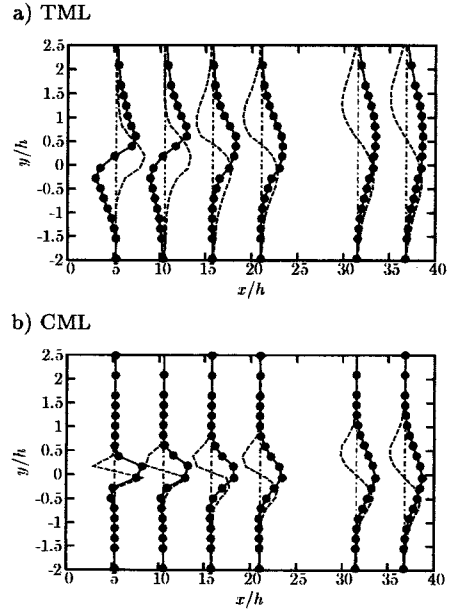


Figure 9: Streamwise evolution of the first two POD modes of the longitudinal velocity component. a) TML, b) CML, —•— first mode, - - - second mode.

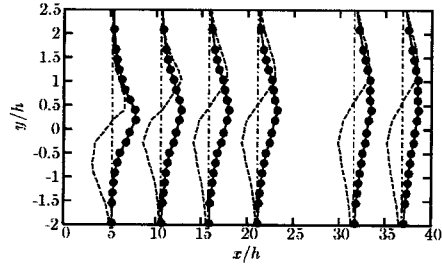


Figure 10: Streamwise evolution of the first two POD modes of the transversal velocity component. TML case, —•— first mode, - - - second mode.

gaussian in form. Thus, in the near region, the POD modes of the thick mixing layer behave like those of a flat plate wake (Delville 1995).

This change of shape of the first two modes with the longitudinal distance is quite similar to that of the Reynolds stress  $\overline{u'v'}$  and can be interpreted as the influence of the wake effect on the shear layer. Considering the behaviour of the  $u$ -component POD modes, the near region is dominated by the wake mode of the flow, and farther downstream, the shear layer tends to behave like a conventionnal mixing layer. The higher order modes of the two kind of flows have the same shape. It appears that only the first two POD modes are modified by the wake influence. This can be interpreted as if the large structures of the flow were strongly altered by the wake of the plate.

The shape of the first two POD modes of the transversal velocity shown in figure 10 do not seem to be affected by the longitudinal evolution of the flow.

Figure 11 shows the longitudinal evolution of the relative importance of the first and the second mode ( $\lambda_1/\lambda_2$ ). The ratio of the first two eigenvalues first decreases with the distance from the trailing edge, reaching a minimum of 1.2 at  $x/h = 15.8$  and then increases. The upstream region is clearly dominated by the first mode which is antisymmetric whereas for  $x/h > 15.8$ , the most energetic mode

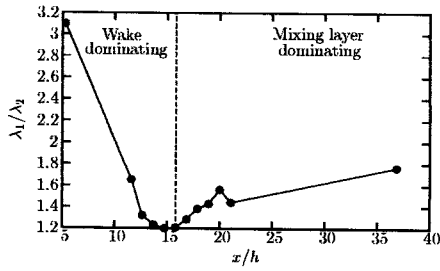


Figure 11: Streamwise evolution of the ratio  $\lambda_1/\lambda_2$  in the TML case.

is symmetric. It should be pointed out that there exists a *transition* region ( $x/h \simeq 15.8$ ) in which the shape of the first two modes change and their corresponding eigenvalues are of the same order of magnitude. Thus, the behaviour of the ratio of the first two eigenvalues reveals where the important modification of the flow organization occurs.

### Spectral POD results

The strong influence of the wake mode in the near region ( $x < 15.8$ ) is also found when a *spectral* POD is computed. The eigenspectra of the POD based on  $u$  in the case of the thick mixing layer are shown in figure 12. At  $x/h = 5.25$ , the first eigenvalue has a strong peak at a frequency  $f$  about 380 Hz. Its first harmonic can also be observed ( $f = 760$  Hz). Spectral analysis of the flow (not presented here) showed that the spectra of the three velocity components exhibit this characteristic frequency in the near region. Downstream ( $x/h = 36.8$ ), the eigenspectra do not present any peak and is closer to the eigenspectra of a conventional mixing layer (see Delville, 1995).

The computation of the POD modes of  $u$  confirms the change of the shape of the first two modes. Figure 13 presents the modulus of the modes weighted by the root of the corresponding eigenvalue. Indeed, at  $x/h = 5.25$  (figure 13 a) and b), the first mode presents two peaks for  $f = 380$  Hz located on each side of the shear layer whereas downstream ( $x/h = 36.8$  figure 13 e) and f)) only one maximum at lower frequencies located on the mixing layer axis can be observed.

Nevertheless, the frequency dependance of the POD modes shows that the transition from a wake dominated flow to a more conventional mixing layer is more progressive than expected from the *spatial* POD mode results. Indeed, at  $x/h = 21$ , the first *spectral* POD mode (see figure 13 c)) exhibits two peaks at the frequency characteristic of the wake Strouhal number ( $f = 380$  Hz) but also a maximum at a lower frequency located on the mixing layer axis (like the first mode at  $x/h = 36.8$ ). At this longitudinal location, the shape of the first *spatial* POD mode is already gaussian, as observed in the beveled trailing edge mixing layer.

### CONCLUSIONS

In the present work, two kind of mixing layers have been investigated: a *conventional* configuration utilizing a splitter plate with a beveled trailing edge and a *thick* mixing layer utilizing a splitter plate with blunt trailing edge which resulted in the interaction of a mixing layer and a wake. The conventional configuration constitutes a reference case to analyse the effect of the dividing plate on the development of the shear layer. The results of this study confirms previous work on the same kind of flow, that is to say the

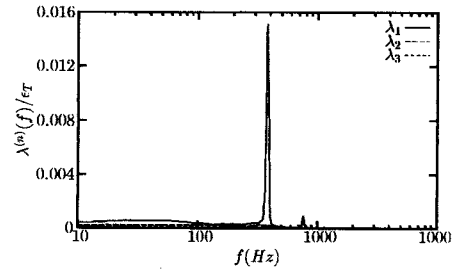


Figure 12: Spectra of the first three eigenvalues. TML case ( $x/h = 36.8$ ).

wake effect produced by the blunt trailing edge modifies the large scale organization. Its influence leads to a streamwise evolution of the flow in which two regions appear: a near wake region clearly dominated by the wake behaviour and a far wake region in which the mixing layer overcome the decreasing wake effect. The POD analysis of the flow field shows that longitudinal evolution strongly affects the large scale structures. Indeed, the first two POD modes which are representative of the most energetic structures in the flow undergo a change in shape with the longitudinal distance from the trailing edge. As regards to the *spatial* POD modes, the transition between the region under the influence of the wake and the far wake region is indicated by the fact that the typical first gaussian-like mode of a classic mixing layer becomes the second mode in the near region and vice versa. In this region, the ratio of the first two eigenvalues  $\lambda_1/\lambda_2$  is minimum and about 1.2. Hence, the flow is not strongly dominated by only one mode in this specific region. Moreover, when a spectral representation of the modes is considered, the first modes and their eigenvalues of the near region exhibit a frequency peak characteristic of the vortex shedding which occurs behind the dividing plate. This frequency corresponds to a Strouhal number based on the trailing edge thickness about 0.24. Downstream, this characteristic frequency progressively disappears as the wake influence is overcome by the mixing layer. Thus, the near wake region plays the role of a strong harmonic excitator of the shear layer as indicated by the modification of the flow organization and the turbulent characteristics.

### ACKNOWLEDGEMENTS

Support of this work has been provided by ONERA under Grant F/10.470/DA-RRAG. First author acknowledges the financial support of the French Ministry of Defense (P. Moschetti). Authors also acknowledge fruitful discussions with Dr. J.J. Allen.

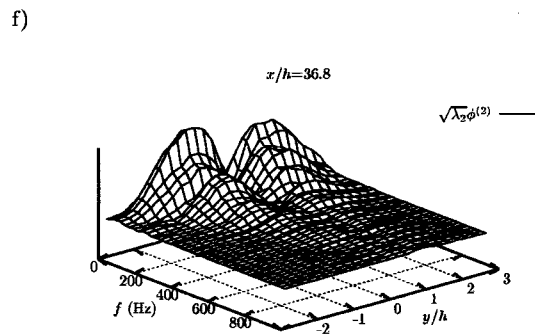
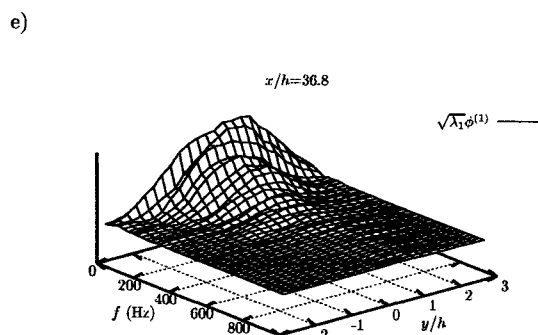
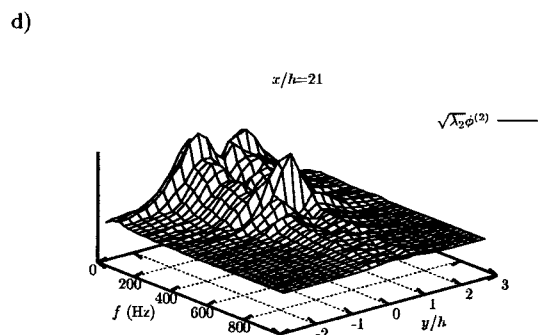
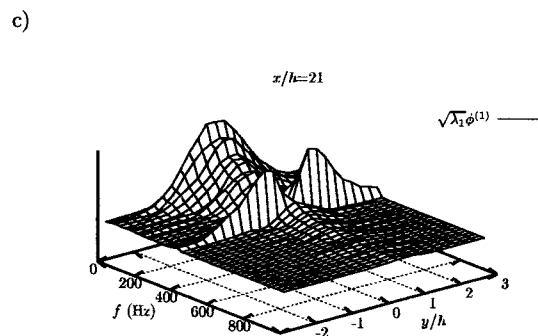
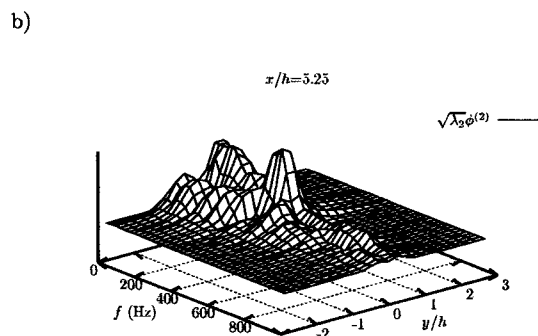
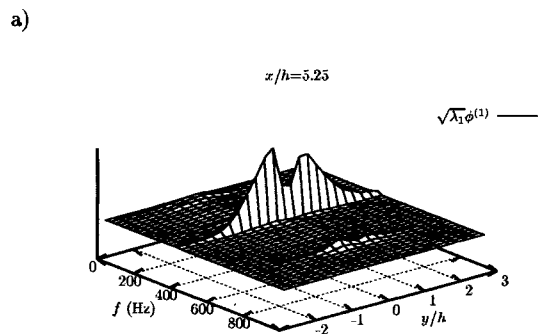


Figure 13: Evolution of the first two modes ( $\sqrt{\lambda_n}\phi^{(n)}$ ) of the longitudinal velocity component obtained by *spectral* POD in the TML case. a) and b):  $x/h=5.25$ , c) and d):  $x/h=21$ , e) and f):  $x/h=36.8$ .(a), c) and e): first mode, b), d) and f): second mode)

#### REFERENCES

- Antonia R.A., 1981, "Conditionnal sampling in turbulence measurement" *Ann. Rev. of Fluid Mech.*, Vol 13, pp. 131-156.
- Aubry N., Guyonnet R. and Lima R., 1991, "Spatiotemporal analysis of complex signals: theory and applications." *J. Stat. Physics*, Vol. 64, pp. 683-739.
- Berkooz G., Holmes P. and Lumley J.L. (1993) "The Proper Orthogonal Decomposition in the analysis of turbulent flows." *Annual Review of Fluid Mech.* Vol 25, pp. 539-575.
- Boldman D.R., Brinich P.F. and Goldstein M.E., 1976, "Vortex shedding from a blunt trailing edge with equal and unequal external mean velocities." *J. Fluid Mech.* Vol. 75, pp. 721-735.
- Delville J., 1995, "La décomposition orthogonale aux valeurs propres et l'analyse de l'organisation tridimensionnelle des écoulements turbulents cisailés libres." , Ph.D. Thesis, University of Poitiers, France.
- Dziomba B. and Fiedler H., 1985, "Effect of initial conditions on two-dimensionnal free shear layers." *J. Fluid Mech.* Vol. 152, pp. 419-442.
- Koch W., 1985, "Local instabilities characteristics and frequency determination of self-excited wake flows." *J. Sound and Vibration* Vol 99, pp. 53-83
- Lumley J.L., 1967, "The Structure of Inhomogeneous Turbulent Flows." *Atm. Turb. and RadioWave Prop.*, Yaglom and Tatarsky eds., *Nauka, Moscow, 166-178.*
- Metha R.D., 1991, "Effect of velocity ratio on plane mixing layer development: Influence of the splitter plate wake." *Exp. Fluids* Vol. 10, pp. 194-204.
- Michalke A. and Schade H., 1965 "Zur stabilitat von freien grenzschichten." *Ing. Arch.* 33, 1.